

ChemComm

Accepted Manuscript



This is an *Accepted Manuscript*, which has been through the Royal Society of Chemistry peer review process and has been accepted for publication.

Accepted Manuscripts are published online shortly after acceptance, before technical editing, formatting and proof reading. Using this free service, authors can make their results available to the community, in citable form, before we publish the edited article. We will replace this *Accepted Manuscript* with the edited and formatted *Advance Article* as soon as it is available.

You can find more information about *Accepted Manuscripts* in the [Information for Authors](#).

Please note that technical editing may introduce minor changes to the text and/or graphics, which may alter content. The journal's standard [Terms & Conditions](#) and the [Ethical guidelines](#) still apply. In no event shall the Royal Society of Chemistry be held responsible for any errors or omissions in this *Accepted Manuscript* or any consequences arising from the use of any information it contains.



Journal Name

COMMUNICATION

A Homochiral Vanadium-Salen-Cadmium bpdc MOF with Permanent Porosity as Asymmetric Catalyst in Solvent-Free Cyanosilylation

Received 00th January 20xx,
Accepted 00th January 20xx

DOI: 10.1039/x0xx00000x

www.rsc.org/

Asamanjoy Bhunia,^a Subarna Dey,^b José María Moreno,^c Urbano Diaz,^c Patricia Concepcion,^c Kristof Van Hecke,^d Christoph Janiak^b and Pascal Van Der Voort^{*a}

A homochiral vanadium-salen based MOF with pcu topology is constructed via *in situ* synthesis under solvothermal conditions. The synthesized MOF exhibits BET surface areas of 574 m²/g, showing the highest H₂ adsorption capacity (1.05 wt % at 77 K, 1 bar) and highest CO₂ uptake (51 cm³/g at 273 K, 1 bar) for currently known salen based MOFs. This framework shows excellent performance as asymmetric catalyst in solvent-free cyanosilylation.

Metal organic frameworks (MOFs) are exciting hybrid materials for a plethora of potential applications including gas storage, gas separation, catalysis, drug delivery.¹⁻³ They are crystalline nanoporous materials comprised of ordered networks formed from organic electron donor linkers and metal cations or clusters.³ In MOF based catalysis, either unsaturated metal coordination sites⁴ or active linker sites in between the metals can be used as the catalytic active sites.^{5,6} This second approach is much more challenging but offers unique opportunities to design highly selective and/or chiral catalysts. The most active linkers have been developed to synthesize the chiral MOFs to date for asymmetric catalysis based on BINOL and salen ligands.⁶⁻⁹

One possible strategy in the synthesis of chiral MOFs is the use of metalloligands.^{7,10-12} In the metalloligand approach, metal-containing homo and heteronuclear complexes (mostly salen types), that exhibit free coordination sites to connect to other metal atoms, are allowed to form 1D, 2D or 3D networks. The additional linkers such as dicarboxylic or bipyridine groups are mostly used to construct a 3D structure that is mostly

responsible for porosity.^{10,11} Since metalloligands are more extended and flexible with respect to traditional organic linkers it is however very hard to stabilize the framework. Although a few MOFs with salen struts have been examined as heterogeneous catalysis or as gas storage/separation vehicle, in most of the cases the framework suffered from severe diffusion limitations, even during the surface area measurements using nitrogen sorption.

Chen *et al.* reported several salen containing MOFs called M'MOFs (mixed-metal organic frameworks) with surface areas ranging from 90-602 m²/g, albeit only measurable by CO₂ uptake at 195 K.^{10,11} The authors argued that the N₂ adsorption at 77 K on the activated M'MOFs was too slow because of diffusion effects. On the other hand, Hupp *et al.* reported that the surface area of the Mn^{III}SO-MOFs and Mn^{II}SO-MOFs was 478 and 385 m²/g using N₂ adsorption at 77 K.¹³

Many examples of asymmetric catalysis have been used by chiral MOFs for the synthesis of chiral molecules while metal centers in the metallosalen linkers are catalytically active. Cui *et al.* reported hydrolytic kinetic resolution and chiral sulfoxidation reactions for Co- and Ti-salen based MOFs respectively, but again the N₂ sorption of their frameworks at 77 K showed only surface adsorption.^{14,15} Hupp and Lin reported Mn- and Ru-salen MOFs for asymmetric catalytic alkenyl epoxidation and cyclopropanation reactions.^{5,12,16} However, these MOFs also did not show permanent porosity. Therefore, the synthesis of permanently porous salen-based chiral frameworks is a huge challenge for asymmetric catalysis and gas sorption within the same frameworks.

In the last few years, one of the most important and rapidly growing concepts is the development of green synthesis methods that are efficient, selective, high yielding and environmentally favorable.^{17,18} Therefore, solvent-free reaction conditions offer significant advantages such as decreased energy consumption, reduced reaction times, less by-product, no purification and a large reduction in reactor size. Also, one-step *in situ* processes save time and consumables. Therefore,

^aDept. of Inorganic and Physical Chemistry, Center for Ordered Materials, Organometallics and Catalysis, Ghent University, Krijgslaan 281-S3, 9000 Ghent, Belgium

^bInstitut für Anorganische Chemie und Strukturchemie, Universität Düsseldorf, 40204 Düsseldorf, Germany

^cInstituto de Tecnología Química (UPV-CSIC), Avenida de los Naranjos s/n, 46022 Valencia, Spain

^dDepartment of Inorganic and Physical Chemistry, Ghent University, Krijgslaan 281-S3, 9000 Ghent, Belgium

*Electronic Supplementary Information (ESI) available: [Experimental details, characterization data, solvent-free cyanosilylation, crystallographic data (CIF), and additional tables and figures]. See DOI: 10.1039/x0xx00000x

situ synthesis as well as solvent-free organic transformation is a great challenge in current research.

Herein, we report a chiral vanadium-salen based Cd-MOF using the chiral ligand (R,R)-(-)-1,2-cyclohexanediamino-N,N'-bis(3-*tert*-butyl-5-(4-pyridyl)salicylidene) (H_2L) via *in situ* synthesis under solvothermal conditions instead of a multi-step¹⁹ process. We tested its potential application in solvent-free cyanosilylation catalysis and its gas adsorption properties.

The reaction of the chiral ligand H_2L , $VOSO_4$, $Cd(NO_3)_2 \cdot (H_2O)_4$ and biphenyl-4,4'-dicarboxylic acid (bpdc) in the presence of DMF/EtOH/ H_2O at 100 °C resulted in the formation of a 3D MOF (see ESI[†] for synthesis and characterization). This compound was characterized by standard analytical/spectroscopic techniques and the solid-state structure was determined by single-crystal X-ray diffraction techniques (Fig. 1). The resulted product is stable in air and insoluble in common organic solvents such as chloroform, acetone, acetonitrile, THF, MeOH, EtOH etc. The bulk purity of the compound was confirmed by comparison of their activated and X-ray diffraction simulated powder (PXRD) patterns (Fig. S2, in ESI[†]). From the thermogravimetric (TG) analysis, it was observed that the activated compound starts to decompose with significant weight loss only above 350 °C (Fig. S3, in ESI[†]).

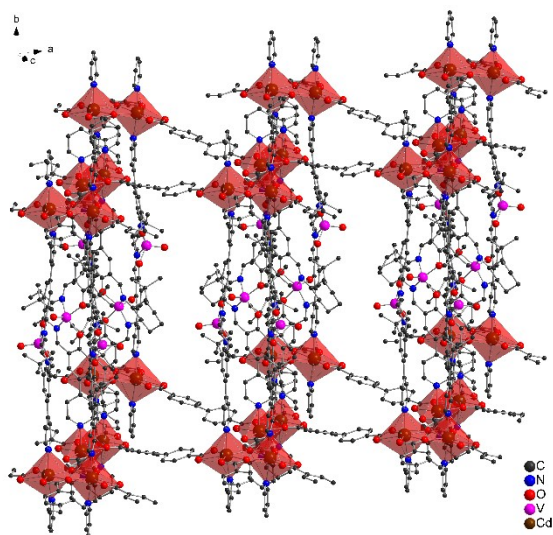


Fig. 1 Section of the packing of V-salen Cd-bpdc MOF from a single-crystal X-ray structure (hydrogen atoms omitted for clarity). Polyhedra depict the edge-sharing pentagonal bipyramidal coordination environment around two adjacent Cd atoms.

The single-crystal X-ray crystallography showed that the compound crystallized in the orthorhombic non-centrosymmetric space group $P222_1$.¹⁹ The asymmetric unit consists of two cadmium(II) ions, two V-salen units ($V^{IV}OL$), and two biphenyldicarboxylate ligands (bpdc). However, both the linkers (VO-salen and bpdc) are parallel to each other in the 1D channel of the framework in which distorted rectangular aperture of $\sim 7 \times 3.5 \text{ \AA}^2$ along the a direction (considering the van der Waals radii of the H and C wall atoms) are estimated, respectively (Fig. S18, ESI[†]). The guest solvent molecules in the channel could not be determined by X-ray crystallography due to their disordered nature, so that the Squeeze option in PLATON was utilized (see details in ESI[†]). Each cadmium(II)

atom is hepta-coordinated by five oxygen atoms from three carboxylate groups of bpdc ligands and two nitrogen atoms from the V-salen pyridine units. Two neighboring cadmium(II) atoms are bridged by two μ_2 - η^2 : η^1 bpdc carboxylate groups to form a secondary building block (SBU) leading to the formation of a 3D network with **pcu** topology (Fig. S16-S17, ESI[†]). In the V-salen unit, oxygen atoms and vanadium(IV) atom are disordered over two positions.^{20,21} As expected, in the center of each salen ligand, the vanadium(IV) atom adopts a distorted square pyramidal coordination geometry. The framework topology was simplified to its underlying net, using the ToposPro program package (see framework topology in ESI[†] for full details).²² The structure shows two equivalent, interpenetrating frameworks (Fig. S11, ESI[†]). In the standard representation, the underlying net of each framework (Fig. S12, ESI[†]) can be considered a 2-nodal 3,5-coordinated net with (3-c)(5-c) nodes stoichiometry, resulting in the formation of a **fet** topology (Fig. S13, ESI[†]), which in the cluster representation, a uninodal 6-coordinated net with the **pcu** topology (Fig. S16, ESI[†]) is observed, with 4 short edges (16.8 Å) and two long, double bridged, opposite (trans) edges (24.0 Å) (running down the [010] direction).

The porosity was characterized by standard N_2 sorption measurements at 77 K. The material was activated by degassing at 100 °C under high vacuum (10^{-6} Torr) for 24 h. The isotherm shows a steep slope at low P/P_0 values with a type I isotherm, which is typical for microporous materials (Fig. 2).^{23,24}

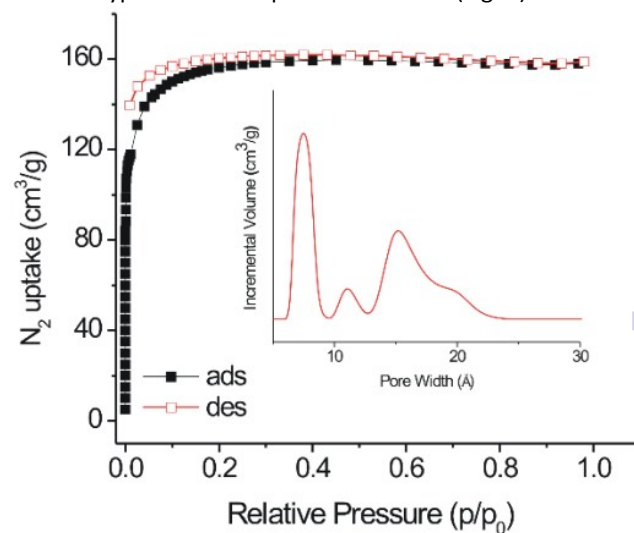


Fig. 2 N_2 sorption isotherm at 77 K. Inset: NL-DFT pore-size distribution curve of V-salen Cd-bpdc MOF.

The calculated Langmuir and BET surface area were found to be 697 and 574 m^2/g , respectively. The total pore volume was estimated as 0.24 cm^3/g at relative pressure $P/P_0 = 0.97$. The absence of hysteresis during the adsorption and desorption points indicated that the framework was stable as well as rigid. To the best of our knowledge, this compound exhibits the highest surface area amongst all metalloligand based MOFs characterized by standard nitrogen sorption (i.e. at 77 K) (Table S1, ESI[†]). Even, the surface area lies in the upper end when compared to other M^IMOFs which showed BET surface areas (measured by CO_2 at 195 K) of 90-602 m^2/g .^{10,11} The pore size distribution was determined by non-local density functional

theory (NL-DFT) using a slit-pore model based on the N₂ adsorption isotherms. A narrow distribution of micropores centered at 7, 11, and 15 Å were observed (insert in Fig. 2). However, the major peak was 7 Å that matches with the calculated value (Fig. S19, ESI[†]), which is obtained from the single-crystal structure (ultramicro-pores <7 Å cannot be detected from N₂ sorption isotherms).

Because of the porosity of the V-salen Cd-bpdc MOF, as well as a large number of nitrogen atoms (imine and pyridine nitrogen atoms) in the framework, we decided to examine its adsorption properties at low pressure (i.e. 1 bar) for CO₂ and other gases (i.e. H₂, CH₄). The CO₂ adsorption capacities in the activated material are 51 cm³/g at 273 K and 32 cm³/g at 298 K (Fig. 3), which is again higher than any known M¹MOFs materials.^{10,11}

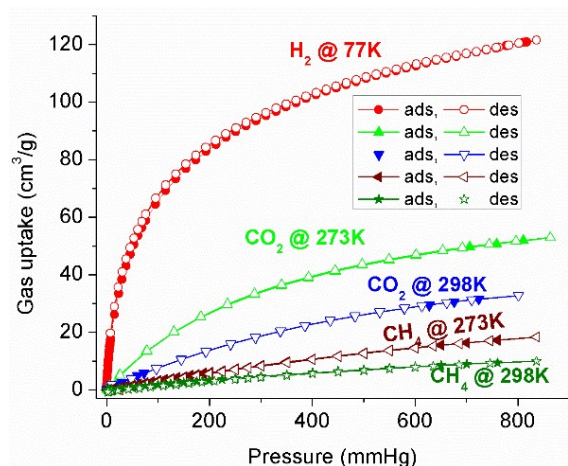


Fig. 3 Low pressure H₂, CO₂ and CH₄ sorption isotherms.

To further understand the adsorption properties, the isosteric heats of adsorption were calculated from the CO₂ adsorption isotherms at 273 K and 298 K (Fig. S4, ESI[†]) as it describes the interaction with the hydrophobic pore surfaces. At zero loading the Q_{st} value (−ΔH) is 30 kJ mol^{−1}. Upon increasing the loading the Q_{st} value decreases rapidly to 28 kJ mol^{−1} which is still well above the heat of liquefaction of bulk CO₂ with 17 kJ mol^{−1} or the isosteric enthalpy of adsorption for CO₂ on activated carbons (e.g. BPL 25.7 kJ mol^{−1}, A10 21.6 kJ mol^{−1}, Norit R1 Extra 22.0 kJ mol^{−1}).^{25,26} The high Q_{st} value can be attributed to the high polar framework and the pore size effect. The high adsorption enthalpy at zero coverage is explained by the initial filling of the small ultramicro-pores with 4 Å diameter (Fig. S5, ESI[†]) with adsorbate–surface interactions to both sides or ends of the CO₂ molecules. In contrast to CO₂, only 17 and 9 cm³/g of nonpolar CH₄ were adsorbed at 273 and 298 K. Interestingly, the material adsorbs 120 cm³/g (or 1.05 wt %) H₂ at 77 K and 1 bar (Fig. 3). This uptake is higher than other M¹MOFs materials, and it is mainly due to size exclusion effects.

We wished to examine if the VO-salen unit is accessible for asymmetric catalytic reactions (Table 1). Therefore, we studied the catalytic activity for cyanosilylation reactions of aromatic aldehydes in solvent-free condition. However, chiral VO-salen complexes are active homogeneous asymmetric catalyst for various type of organic reactions.²⁷ To optimize the reaction conditions, the study was carried out in the reaction of

benzaldehyde (0.82 mmol) and trimethylsilyl cyanide (2.46 mmol) by using 0.25 mol % catalyst with N₂ atmosphere at 30 °C. The resulting yield of the reaction reached up to 95 % after 14 h. Upon increasing the time, the yield of the reaction did not improve, being the cyanosilylation reaction performed with a 1:3 mol ratio of the selected aldehyde and TMS-CN with N₂ atmosphere at 30 °C for 14 h as optimal working conditions (Fig. S6, ESI[†]). To confirm the leaching, the catalyst is separated by filtration or centrifugation when the yield reached 35 % and then the reaction was continued (hot filtration test) (Fig. S6, ESI[†]). After 14 h, we observed that the reaction yield did not increase further.

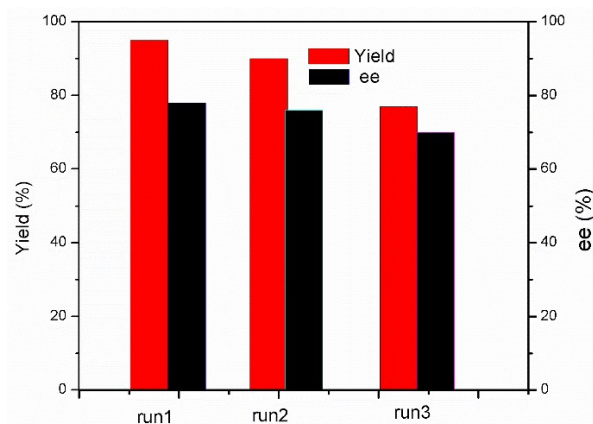


Fig. 4 Yield and enantiomeric excess (ee) for cyanosilylation reaction of benzaldehyde during 1st, 2nd and 3rd run.

Table 1 Asymmetric cyanosilylation of aldehydes catalyzed by vanadium-salen Cd-bpdc MOF^a

Entry	R	Time	Yield (%) ^b	ee (%) ^c
1	H	14	95	78
2	Me	14	93	76
3	OMe	14	76	80
4	Cl	14	98	72
5	Br	14	98	76
6 ^d	H	9	91	57

^aReaction condition: Catalyst (0.25 mol%), aldehyde (0.87 mmol) and trimethylsilyl cyanide (3 eq), time 14 h. ^bCalculated by GC. ^cDetermined by chiral GC. ^dCatalyzed by VO-salen in homogeneous phase.

MOF materials are structured from coordination bonds between metallic clusters and organic ligands which can be easily modified in contact with organic solvents. In fact, leaching phenomena are frequently observed when solid MOFs catalysts are used in different catalytic processes. In our case, the use of solvent-free conditions, during the cyanosilylation of aldehyde, favors the preservation of the V-salen-MOF structure, avoiding the decomposition and disorganization of the pristine MOF, and preventing the presence of homogeneous active sites in the

reaction media. Experiments carried out in presence of different solvents (chloroform, acetonitrile) confirmed this fact because leaching is clearly detected, showing the convenience to avoid the use of the organic solvents during the catalytic processes (Fig. S10a-S10b in ESI). Further, chiral centers are influenced by their chemical environment. The presence of organic solvents as reaction medium together with the hydrophobic properties of MOF materials could favor the excessive presence of solvent molecules adsorbed around chiral active sites. The consequence could be an activity decrease of asymmetric centers. Considering this, solvent-free conditions would be preferred for chiral solid catalysts. Therefore, we investigated the catalytic reaction in absence of any solvent. Under these optimized conditions, cyanosilylation of benzaldehyde gave 95 % yield with 78 % *ee* (Fig. 4, and Table 1), which is highly compared with the recent work from the Duan and Cui groups.^{28,19} They carried out heterogeneous asymmetric cyanosilylation reaction by using an organic solvent such as CH₃CN and DCM. Even, the Cui group used Ph₃PO as a base to promote cyanosilylation.¹⁹ To the best of our knowledge, no solvent-free cyanosilylation has been reported for salen based MOFs. In our study, we not only use solvent-free conditions but also less amount of catalyst. Moreover, the heterogeneous nature of the reaction was further confirmed by recyclability and reusability tests of the catalyst in cyanosilylation of benzaldehyde (Fig. 4, and Fig. S6-S7 in ESI†). We observed that the activity was maintained for the following two runs without significant change of *ee* (Fig. 4, Table S2). In the 3rd run, the yield and *ee* were decreased, which is associated to modification of surrounding environment of chiral centers or undesirable adsorption of organic compounds. After the 3rd run, the catalyst still maintained its crystalline structure which was confirmed by PXRD (Fig. S7, ESI†). Moreover, the UV-vis spectrum of fresh and reused catalyst (after the 3rd run) did not show remarkable changes in the vanadium species (Fig. S7, ESI†). In order to prove the effect of introducing different substituents in the aromatic ring at the *para* position, we further used aromatic aldehydes with an electron-withdrawing (-Cl and -Br) and electron-donating (-Me and -OMe) group (Table 1 and Fig. S8 in ESI†). The electron-withdrawing (-Cl and -Br) group gave higher yield whereas the electron-donating groups decreased the yield with respect to benzaldehyde. This tendency is explained by the higher electropositive charge on the carbonyl group of aldehyde achieved in presence of electron-withdrawing groups, resulting in higher activation of the substrate. On the contrary, with electron-donating groups, the activation of carbonyl group is lower. Moreover, in all cases the *ee* is higher than 72% (Table 1).

In conclusion, we have reported a chiral vanadium-salen Cd-bpdc MOF using a chiral salen ligand (R,R)-(-)-1,2-cyclohexanediamino-N,N'-bis(3-*tert*-butyl-5-(4-pyridyl)salicylidene (H₂L) via *in situ* synthesis under solvothermal conditions. This MOF shows to be an intrinsically microporous with a high BET surface area of 574 m²/g. At 273 K and 1 bar, this framework exhibits a higher CO₂ uptake capacity than other metallosalen-based MOFs. We tested this

compound as a chiral catalyst for asymmetric cyanosilylation of aromatic aldehydes under solvent-free condition. The catalyst is recyclable and reusable and showed a good conversion and *ee*. This green and solvent-free approach can be highly suitable for the synthesis of various chiral products such as α -hydroxy acids, α -hydroxy aldehydes and β -amino alcohols through corresponding cyanohydrin in biomedical chemistry.

This research is funded by Ghent University, GOA grant number 01G00710.

Notes and references

† Crystal data for **V-salen Cd-bpdc MOF**: C₁₀₄H₁₀₀Cd₂N₈O_{13.63}V₂, M = 2006.6, orthorhombic, space group P2221 (No. 17), a = 17.0460(5), b = 24.0462(6) Å, c = 28.8442(6) Å, V = 11823.0(5) Å³, Z = 4, T = 100 K, $\rho_{\text{calc}} = 1.127 \text{ g cm}^{-3}$, $\mu(\text{Cu-K}\alpha) = 4.565 \text{ mm}^{-1}$, F(000) = 4124.1, 68492 reflections measured, 24063 unique ($R_{\text{int}} = 0.092$) which were used in all calculations. The final R1 was 0.0564 ($I > 2\sigma(I)$) and wR2 was 0.1393 (all data). CCDC 1422004

- H. Furukawa, K. E. Cordova, M. O'Keeffe and O. M. Yaghi, *Science*, 2013, **320**, 1230-1234.
- K. Sumida, D. L. Rogow, J. A. Mason, T. M. McDonald, E. D. Bloch, Z. R. Herm, T.-H. Bae and J. R. Long, *Chem. Rev.*, 2012, **112**, 724-781.
- G. Férey, *Chem. Soc. Rev.*, 2008, **37**, 191-214.
- A. Corma, H. García and F. X. Llabrés i Xamena, *Chem. Rev.*, 2010, **110**, 4607-4655.
- S.-H. Cho, B. Ma, S. T. Nguyen, J. T. Hupp and T. E. Albrecht-Schmitt, *Chem. Commun.*, 2006, 2563-2565.
- L. Ma, J. M. Falkowski, C. Abney and W. Lin, *Nat. Chem.*, 2010, **2**, 838-846.
- R. Kitaura, G. Onoyama, H. Sakamoto, R. Matsuda, S.-I. Noro and M. Kitagawa, *Angew. Chem. Int. Ed.*, 2004, **43**, 2684-2687.
- A. Bhunia, Y. Lan, V. Mereacre, M. T. Gamer, A. K. Powell and P. W. Roesky, *Inorg. Chem.*, 2011, **50**, 12697-12704.
- A. Bhunia, M. A. Gotthardt, M. Yadav, M. T. Gamer, A. Eichhöfer, W. Kleist and P. W. Roesky, *Chem. – Eur. J.*, 2013, **19**, 1986-1995.
- S.-C. Xiang, Z. Zhang, C.-G. Zhao, K. Hong, X. Zhao, D.-R. Ding, M.-H. Xie, C. D. Wu, M. C. Das, R. Gill, K. M. Thomas and B. Chen, *Nat. Commun.*, 2011, **2**, 204.
- M. C. Das, Q. Guo, Y. He, J. Kim, C.-G. Zhao, K. Hong, S. Xiang, Z. Zhang, K. M. Thomas, R. Krishna and B. Chen, *J. Am. Chem. Soc.*, 2012, **134**, 8703-8710.
- F. Song, C. Wang, J. M. Falkowski, L. Ma and W. Lin, *J. Am. Chem. Soc.*, 2012, **134**, 15390-15398.
- A. M. Shultz, A. A. Sarjeant, O. K. Farha, J. T. Hupp and S. T. Nguyen, *J. Am. Chem. Soc.*, 2011, **133**, 13252-13255.
- C. Zhu, G. Yuan, X. Chen, Z. Yang and Y. Cui, *J. Am. Chem. Soc.*, 2012, **134**, 8058-8061.
- W. Xuan, C. Ye, M. Zhang, Z. Chen and Y. Cui, *Chem. Sci.*, 2013, **4**, 3154-3159.
- J. M. Falkowski, C. Wang, S. Liu and W. Lin, *Angew. Chem. Int. Ed.*, 2011, **50**, 8674-8678.
- J. M. DeSimone, *Science*, 2002, **297**, 799-803.
- P. J. Walsh, H. Li and C. A. de Parrodi, *Chem. Rev.*, 2007, **107**, 2503-2545.
- W. Xi, Y. Liu, Q. Xia, Z. Li and Y. Cui, *Chem. – Eur. J.*, 2015, **21**, 12581-12585.
- Y. N. Belokon, P. Carta, A. V. Gutnov, V. Maleev, M. A. Moskalenko, L. Yashkina, N. S. Ikonnikov, N. V. Voskoboev, V. N. Khrestalev and M. North, *Helv. Chim. Acta*, 2002, **85**, 3301-3312.
- P. Adão, J. Costa Pessoa, R. T. Henriques, M. L. Kuznetsov, F. Avecilla, M. Maurya, U. Kumar and I. Correia, *Inorg. Chem.*, 2009, **48**, 3542-3561.
- V. A. Blatov, A. P. Shevchenko and D. M. Proserpio, *Cryst. Growth Des.*, 2003, **3**, 3576-3586.
- K. S. W. Sing, D. H. Everett, R. A. W. Haul, L. Moscou, R. A. Pierotti, J. Rouquerol and T. Siemieniowska, *Pure Appl. Chem.*, 1985, **57**, 603-610.
- G. Loufanti, M. Padovan, G. Tozzola and B. Venturelli, *Catal. Today*, 1998, **41**, 207-219.
- K. B. Lee, M. G. Beaver, H. S. Caram and S. Sircar, *Ind. Eng. Chem. Res.*, 2006, **47**, 8048-8062.
- S. Himeno, T. Komatsu and S. Fujita, *J. Chem. Eng. Data*, 2005, **50**, 369-371.
- (a) V. Chechik, M. Conte, T. Dransfield, M. North and M. Omedes-Pujol, *Chem. Commun.*, 2010, **46**, 3372-3374; (b) Y. N. Belokon, M. North and T. Parsons, *Org. Lett.*, 2000, **2**, 1617-1619.
- D. Dang, P. Wu, C. He, Z. Xie and C. Duan, *J. Am. Chem. Soc.*, 2010, **132**, 14321-14323.



Journal Name

COMMUNICATION

A Homochiral Vanadium-Salen-Cadmium bpdc MOF with Permanent Porosity as Asymmetric Catalyst in Solvent-Free Cyanosilylation

Received 00th January 20xx,
Accepted 00th January 20xx

DOI: 10.1039/x0xx00000x

www.rsc.org/

Asamanjoy Bhunia,^a Subarna Dey,^b José María Moreno,^c Urbano Diaz,^c Patricia Concepcion,^c Kristof Van Hecke,^d Christoph Janiak^b and Pascal Van Der Voort^{*a}

A homochiral vanadium-salen based MOF with pcu topology is constructed via *in situ* synthesis under solvothermal conditions. The synthesized MOF exhibits BET surface areas of 574 m²/g, showing the highest H₂ adsorption capacity (1.05 wt % at 77 K, 1 bar) and highest CO₂ uptake (51 cm³/g at 273 K, 1 bar) for currently known salen based MOFs. This framework shows excellent performance as asymmetric catalyst in solvent-free cyanosilylation.

Metal organic frameworks (MOFs) are exciting hybrid materials for a plethora of potential applications including gas storage, gas separation, catalysis, drug delivery.¹⁻³ They are crystalline nanoporous materials comprised of ordered networks formed from organic electron donor linkers and metal cations or clusters.³ In MOF based catalysis, either unsaturated metal coordination sites⁴ or active linker sites in between the metals can be used as the catalytic active sites.^{5,6} This second approach is much more challenging but offers unique opportunities to design highly selective and/or chiral catalysts. The most active linkers have been developed to synthesize the chiral MOFs to date for asymmetric catalysis based on BINOL and salen ligands.⁶⁻⁹

One possible strategy in the synthesis of chiral MOFs is the use of metalloligands.^{7,10-12} In the metalloligand approach, metal-containing homo and heteronuclear complexes (mostly salen types), that exhibit free coordination sites to connect to other metal atoms, are allowed to form 1D, 2D or 3D networks. The additional linkers such as dicarboxylic or bipyridine groups are mostly used to construct a 3D structure that is mostly

responsible for porosity.^{10,11} Since metalloligands are more extended and flexible with respect to traditional organic linkers, it is however very hard to stabilize the framework. Although a few MOFs with salen struts have been examined as heterogeneous catalysis or as gas storage/separation vehicle, in most of the cases the framework suffered from severe diffusion limitations, even during the surface area measurements using nitrogen sorption.

Chen *et al.* reported several salen containing MOFs called M'MOFs (mixed-metal organic frameworks) with surface areas ranging from 90-602 m²/g, albeit only measurable by CO₂ uptake at 195 K.^{10,11} The authors argued that the N₂ adsorption at 77 K on the activated M'MOFs was too slow because of diffusion effects. On the other hand, Hupp *et al.* reported that the surface area of the Mn^{III}SO-MOFs and Mn^{II}SO-MOFs was 478 and 385 m²/g using N₂ adsorption at 77 K.¹³

Many examples of asymmetric catalysis have been used by chiral MOFs for the synthesis of chiral molecules while metal centers in the metallosalen linkers are catalytically active. Cui *et al.* reported hydrolytic kinetic resolution and chiral sulfoxidation reactions for Co- and Ti-salen based MOFs, respectively, but again the N₂ sorption of their frameworks at 77 K showed only surface adsorption.^{14,15} Hupp and Lin reported Mn- and Ru-salen MOFs for asymmetric catalytic alkene epoxidation and cyclopropanation reactions.^{5,12,16} However, these MOFs also did not show permanent porosity. Therefore, the synthesis of permanently porous salen-based chiral frameworks is a huge challenge for asymmetric catalysis and gas sorption within the same frameworks.

In the last few year, one of the most important and rapidly growing concepts is the development of green synthesis methods that are efficient, selective, high yielding and environmentally favorable.^{17,18} Therefore, solvent-free reaction conditions offer significant advantages such as decreased energy consumption, reduced reaction times, less by-products, no purification and a large reduction in reactor size. Also, one-step *in situ* processes save time and consumables. Therefore, *in situ* synthesis as well as solvent-

^a Dept. of Inorganic and Physical Chemistry, Center for Ordered Materials, Organometallics and Catalysis, Ghent University, Krijgslaan 281-S3, 9000 Ghent, Belgium

^b Institut für Anorganische Chemie und Strukturchemie, Universität Düsseldorf, 40204 Düsseldorf, Germany

^c Instituto de Tecnología Química (UPV-CSIC), Avenida de los Naranjos s/n, 46022 Valencia, Spain

^d Department of Inorganic and Physical Chemistry, Ghent University, Krijgslaan 281-S3, 9000 Ghent, Belgium

*Electronic Supplementary Information (ESI) available: [Experimental details, characterization data, solvent-free cyanosilylation, crystallographic data (CIF), and additional tables and figures]. See DOI: 10.1039/x0xx00000x

free organic transformation is a great challenge in current research.

Herein, we report a chiral vanadium-salen based Cd-MOF using the chiral ligand (R,R)-(-)-1,2-cyclohexanediamino-N,N'-bis(3-*tert*-butyl-5-(4-pyridyl)salicylidene) (H_2L) via *in situ* synthesis under solvothermal conditions instead of a multi-step¹⁹ process. We tested its potential application in solvent-free cyanosilylation catalysis and its gas adsorption properties.

The reaction of the chiral ligand H_2L , $VOSO_4$, $Cd(NO_3)_2 \cdot (H_2O)_4$ and biphenyl-4,4'-dicarboxylic acid (bpdc) in the presence of DMF/EtOH/ H_2O at 100 °C resulted in the formation of a 3D MOF (see ESI[†] for synthesis and characterization). This compound was characterized by standard analytical/spectroscopic techniques and the solid-state structure was determined by single-crystal X-ray diffraction techniques (Fig. 1). The resulted product is stable in air and insoluble in common organic solvents such as chloroform, acetone, acetonitrile, THF, MeOH, EtOH etc. The bulk purity of the compound was confirmed by comparison of their activated and X-ray diffraction simulated powder (PXRD) patterns (Fig. S2, in ESI[†]). From the thermogravimetric (TG) analysis, it was observed that the activated compound starts to decompose with significant weight loss only above 350 °C (Fig. S3, in ESI[†]).

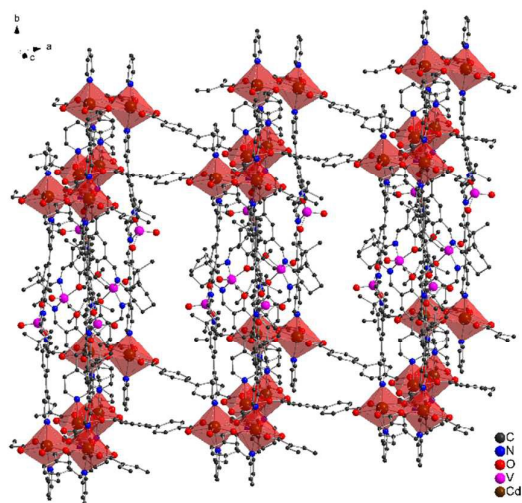


Fig. 1 Section of the packing of V-salen Cd-bpdc MOF from a single-crystal X-ray structure (hydrogen atoms omitted for clarity). Polyhedra depict the edge-sharing pentagonal bipyramidal coordination environment around two adjacent Cd atoms.

The single-crystal X-ray crystallography showed that the compound crystallized in the orthorhombic non-centrosymmetric space group $P222_1$.¹⁹ The asymmetric unit consists of two cadmium(II) ions, two V-salen units ($V^{IV}OL$), and two biphenyldicarboxylate ligands (bpdc). However, both the linkers (VO-salen and bpdc) are parallel to each other in the 1D channel of the framework in which distorted rectangular aperture of $\sim 7 \times 3.5 \text{ \AA}^2$ along the a direction (considering the van der Waals radii of the H and C wall atoms) are estimated, respectively (Fig. S18, ESI[†]). The guest solvent molecules in the channel could not be determined by X-ray crystallography due to their disordered nature, so that the Squeeze option in

PLATON was utilized (see details in ESI[†]). Each cadmium(II) atom is hepta-coordinated by five oxygen atoms from three carboxylate groups of bpdc ligands and two nitrogen atoms from the V-salen pyridine units. Two neighboring cadmium(II) atoms are bridged by two $\mu_2-\eta^2:\eta^1$ bpdc carboxylate groups and form a secondary building block (SBU) leading to the formation of a 3D network with **pcu** topology (Fig. S16-S17, ESI[†]). In the V-salen unit, oxygen atoms and vanadium(IV) atom are disordered over two positions.^{20,21} As expected, in the center of each salen ligand, the vanadium(IV) atom adopts a distorted square pyramidal coordination geometry. The framework topology was simplified to its underlying net, using the ToposPro program package (see framework topology in ESI[†] for full details).²² The structure shows two equivalent, interpenetrating frameworks (Fig. S11, ESI[†]). In the standard representation, the underlying net of each framework (Fig. S12, ESI[†]) can be considered a 2-nodal 3,5-coordinated net with (3-c)(5-c) nodes stoichiometry, resulting in the formation of a **fet** topology (Fig. S13, ESI[†]), while in the cluster representation, a uninodal 6-coordinated net with the **pcu** topology (Fig. S16, ESI[†]) is observed, with 4 short edges (16.8 Å) and two long, double bridged, opposite (trans) edges (24.0 Å) (running down the [010] direction).

The porosity was characterized by standard N_2 sorption measurements at 77 K. The material was activated by degassing at 100 °C under high vacuum (10^{-6} Torr) for 24 h. The isotherm shows a steep slope at low P/P_0 values with a type I isotherm which is typical for microporous materials (Fig. 2).^{23,24}

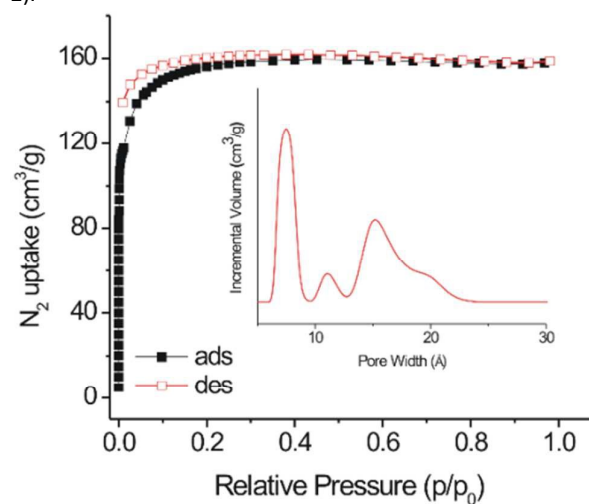


Fig. 2 N_2 sorption isotherm at 77 K. Inset: NL-DFT pore-size distribution curve of V-salen Cd-bpdc MOF.

The calculated Langmuir and BET surface area were found to be 697 and 574 m^2/g , respectively. The total pore volume was estimated as 0.24 cm^3/g at relative pressure $P/P_0 = 0.97$. The absence of hysteresis during the adsorption and desorption points indicated that the framework was stable as well as rigid. To the best of our knowledge, this compound exhibits the highest surface area amongst all metalloligand based MOFs characterized by standard nitrogen sorption (i.e. at 77 K) (Table S1, ESI[†]). Even, the surface area lies in the upper end

when compared to other M¹MOFs which showed BET surface areas (measured by CO₂ at 195 K) of 90–602 m²/g.^{10,11} The pore size distribution was determined by non-local density functional theory (NL-DFT) using a slit-pore model based on the N₂ adsorption isotherms. A narrow distribution of micropores centered at 7, 11, and 15 Å were observed (insert in Fig. 2). However, the major peak was 7 Å that matches with the calculated value (Fig. S19, ESI[†]), which is obtained from the single-crystal structure (ultramicropores <7 Å cannot be detected from N₂ sorption isotherms).

Because of the porosity of the V-salen Cd-bpdc MOF, as well as a large number of nitrogen atoms (imine and pyridine nitrogen atoms) in the framework, we decided to examine its adsorption properties at low pressure (i.e. 1 bar) for CO₂ and other gases (i.e. H₂, CH₄). The CO₂ adsorption capacities in the activated material are 51 cm³/g at 273 K and 32 cm³/g at 298 K (Fig. 3), which is again higher than any known M¹MOFs materials.^{10,11}

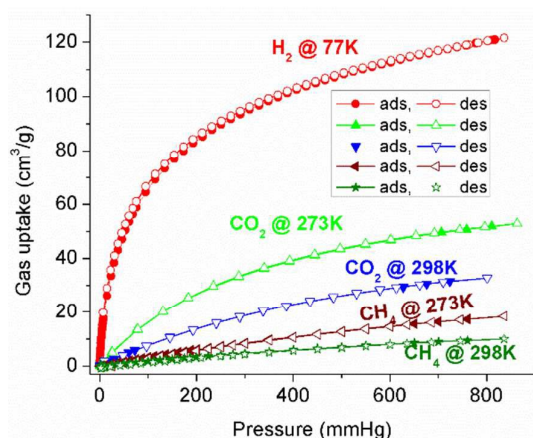


Fig. 3 Low pressure H₂, CO₂ and CH₄ sorption isotherms.

To further understand the adsorption properties, the isosteric heats of adsorption were calculated from the CO₂ adsorption isotherms at 273 K and 298 K (Fig. S4, ESI[†]) as it describes the interaction with the hydrophobic pore surfaces. At zero loading the Q_{st} value (−ΔH) is 30 kJ mol^{−1}. Upon increasing the loading the Q_{st} value decreases rapidly to 28 kJ mol^{−1} which is still well above the heat of liquefaction of bulk CO₂ with 17 kJ mol^{−1} or the isosteric enthalpy of adsorption for CO₂ on activated carbons (e.g. BPL 25.7 kJ mol^{−1}, A10 21.6 kJ mol^{−1}, Norit R1 Extra 22.0 kJ mol^{−1}).^{25,26} The high Q_{st} value can be attributed to the high polar framework and the pore size effect. The high adsorption enthalpy at zero coverage is explained by the initial filling of the small ultramicropores with 4 Å diameter (Fig. S5, ESI[†]) with adsorbate–surface interactions to both sides or ends of the CO₂ molecules. In contrast to CO₂, only 17 and 9 cm³/g of nonpolar CH₄ were adsorbed at 273 and 298 K. Interestingly, the material adsorbs 120 cm³/g (or 1.05 wt %) H₂ at 77 K and 1 bar (Fig. 3). This uptake is higher than other M¹MOFs materials, and it is mainly due to size exclusion effects.

We wished to examine if the VO-salen unit is accessible for asymmetric catalytic reactions (Table 1). Therefore, we studied the catalytic activity for cyanosilylation reactions of aromatic

aldehydes in solvent-free condition. However, chiral VO-salen complexes are active homogeneous asymmetric catalyst for various type of organic reactions.²⁷ To optimize the reaction conditions, the study was carried out in the reaction of benzaldehyde (0.82 mmol) and trimethylsilyl cyanide (2.46 mmol) by using 0.25 mol % catalyst with N₂ atmosphere at 30 °C. The resulting yield of the reaction reached up to 95 % after 14 h. Upon increasing the time, the yield of the reaction did not improve, being the cyanosilylation reaction performed with a 1:3 mol ratio of the selected aldehyde and TMSCN with N₂ atmosphere at 30°C for 14 h as optimal working conditions (Fig. S6, ESI[†]). To confirm the leaching, the catalyst is separated by filtration or centrifugation when the yield reached 35 % and then the reaction was continued (hot filtration test) (Fig. S6, in ESI[†]). After 14 h, we observed that the reaction yield did not increase further.

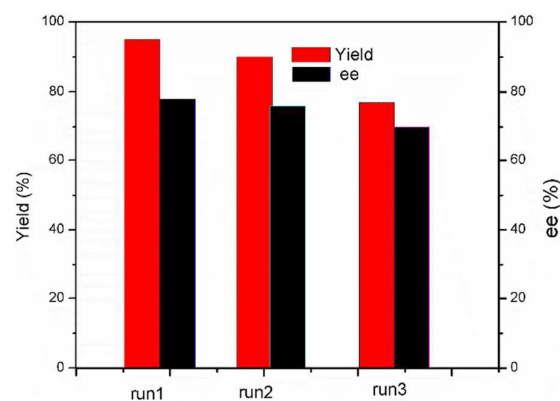


Fig. 4 Yield and enantiomeric excess (ee) for cyanosilylation reaction of benzaldehyde during 1st, 2nd and 3rd run.

Table 1 Asymmetric cyanosilylation of aldehydes catalyzed by vanadium-salen Cd-bpdc MOF^a

Entry	R	Time	Yield (%) ^b	ee (%) ^c
1	H	14	95	78
2	Me	14	93	76
3	OMe	14	76	80
4	Cl	14	98	72
5	Br	14	98	76
6 ^d	H	9	91	57

^aReaction condition: Catalyst (0.25 mol%), aldehyde (0.87 mmol) and trimethylsilyl cyanide (3 eq), time 14 h.^bCalculated by GC. ^cDetermined by chiral GC. ^dCatalyst: VO-salen in homogeneous phase.

MOF materials are structured from coordination bonds between metallic clusters and organic ligands which can be easily modified in contact with organic solvents. In fact, leaching phenomena are frequently observed when solid MOFs catalysts are used in different catalytic processes. In our

case, the use of solvent-free conditions, during the cyanosilylation of aldehydes, favors the preservation of the V-salen-MOF structure, avoiding the decomposition and disorganization of the pristine MOF, and preventing the presence of homogeneous active sites in the reaction media. Experiments carried out in presence of different solvents (chloroform, acetonitrile) confirmed this fact because leaching is clearly detected, showing the convenience to avoid the use of the organic solvents during the catalytic processes (Fig. S10a-S10b in ESI). Further, chiral centers are influenced by their chemical environment. The presence of organic solvents as reaction medium together with the hydrophobic properties of MOF materials could favor the excessive presence of solvent molecules adsorbed around chiral active sites. The consequence could be an activity decrease of asymmetric centers. Considering this, solvent-free conditions would be preferred for chiral solid catalysts. Therefore, we investigated the catalytic reaction in absence of any solvent. Under these optimized conditions, cyanosilylation of benzaldehyde gave 95 % yield with 78 % *ee* (Fig. 4, and Table 1), which is highly compared with the recent work from the Duan and Cui groups.^{28,19} They carried out heterogeneous asymmetric cyanosilylation reaction by using an organic solvent such as CH₃CN and DCM. Even, the Cui group used Ph₃PO as a base to promote cyanosilylation.¹⁹ To the best of our knowledge, no solvent-free cyanosilylation has been reported for salen based MOFs. In our study, we not only use solvent-free conditions but also less amount of catalyst. Moreover, the heterogeneous nature of the reaction was further confirmed by recyclability and reusability tests of the catalyst in cyanosilylation of benzaldehyde (Fig. 4, and Fig. S6-S7 in ESI[†]). We observed that the activity was maintained for the following two runs without significant change of *ee* (Fig. 4, Table S2). In the 3rd run, the yield and *ee* were decreased, which is associated to modification of surrounding environment of chiral centers or undesirable adsorption of organic compounds. After the 3rd run, the catalyst still maintained its crystalline structure which was confirmed by PXRD (Fig. S7, ESI[†]). Moreover, the UV-vis spectrum of fresh and reused catalyst (after the 3rd run) did not show remarkable changes in the vanadium species (Fig. S7, ESI[†]). In order to prove the effect of introducing different substituents in the aromatic ring at the *para* position, we further used aromatic aldehydes with an electron-withdrawing (-Cl and -Br) and electron-donating (-Me and -OMe) group (Table 1 and Fig. S8 in ESI[†]). The electron-withdrawing (-Cl and -Br) group gave higher yield whereas the electron-donating groups decreased the yield with respect to benzaldehyde. This tendency is explained by the higher electropositive charge on the carbonyl group of aldehyde achieved in presence of electron-withdrawing groups, resulting in higher activation of the substrate. On the contrary, with electron-donating groups, the activation of carbonyl group is lower. Moreover, in all cases the *ee* is higher than 72% (Table 1).

In conclusion, we have reported a chiral vanadium-salen Cd-bpdc MOF using a chiral salen ligand (R,R)-(-)-1,2-cyclohexanediamino-N,N'-bis(3-*tert*-butyl-5-(4-

pyridyl)salicylidene (H₂L) via *in situ* synthesis under solvothermal conditions. This MOF shows to be a intrinsically microporous with a high BET surface area of 574 m²/g. At 273 K and 1 bar, this framework exhibits a higher CO₂ uptake capacity than other metallosalen-based MOFs. We tested this compound as a chiral catalyst for asymmetric cyanosilylation of aromatic aldehydes under solvent-free condition. The catalyst is recyclable and reusable and showed a good conversion and *ee*. This green and solvent-free approach can be highly suitable for the synthesis of various chiral products such as α -hydroxy acids, α -hydroxy aldehydes and β -amino alcohols through corresponding cyanohydrin in biomedicinal chemistry.

This research is funded by Ghent University, GOA grant number 01G00710.

Notes and references

† Crystal data for V-salen Cd-bpdc MOF: C₁₀₄H₁₀₀Cd₂N₈O₁₃₋₆₃V₂, M = 2006.69, orthorhombic, space group P2221 (No. 17), a = 17.0460(5), b = 24.0462(6) Å, c = 28.8442(6) Å, V = 11823.0(5) Å³, Z = 4, T = 100 K, $\rho_{\text{calc}} = 1.127 \text{ g cm}^{-3}$, $\mu(\text{Cu-K}\alpha) = 4.565 \text{ mm}^{-1}$, F(000) = 4124.1, 68492 reflections measured, 24063 unique ($R_{\text{int}} = 0.0926$) which were used in all calculations. The final R1 was 0.0564 ($I > 2\sigma(I)$) and wR2 was 0.1393 (all data). CCDC 1422004

- H. Furukawa, K. E. Cordova, M. O'Keeffe and O. M. Yaghi, *Science*, 2013, **341**, 1230444.
- K. Sumida, D. L. Rogow, J. A. Mason, T. M. McDonald, E. D. Bloch, Z. R. Herm, T.-H. Bae and J. R. Long, *Chem. Rev.*, 2012, **112**, 724-781.
- G. Férey, *Chem. Soc. Rev.*, 2008, **37**, 191-214.
- A. Corma, H. Garcia and F. X. Llabrés i Xamena, *Chem. Rev.*, 2010, **110**, 4606-4655.
- S.-H. Cho, B. Ma, S. T. Nguyen, J. T. Hupp and T. E. Albrecht-Schmitt, *Chem. Commun.*, 2006, 2563-2565.
- L. Ma, J. M. Falkowski, C. Abney and W. Lin, *Nat. Chem.*, 2010, **2**, 838-846.
- R. Kitaura, G. Onoyama, H. Sakamoto, R. Matsuda, S.-I. Noro and S. Kitagawa, *Angew. Chem. Int. Ed.*, 2004, **43**, 2684-2687.
- A. Bhunia, Y. Lan, V. Mereacre, M. T. Gamer, A. K. Powell and P. W. Roesky, *Inorg. Chem.*, 2011, **50**, 12697-12704.
- A. Bhunia, M. A. Gotthardt, M. Yadav, M. T. Gamer, A. Eichhöfer, W. Kleist and P. W. Roesky, *Chem. – Eur. J.*, 2013, **19**, 1986-1995.
- S.-C. Xiang, Z. Zhang, C.-G. Zhao, K. Hong, X. Zhao, D.-R. Ding, M.-H. Xie, C.-D. Wu, M. C. Das, R. Gill, K. M. Thomas and B. Chen, *Nat. Commun.*, 2011, **2**, 204.
- M. C. Das, Q. Guo, Y. He, J. Kim, C.-G. Zhao, K. Hong, S. Xiang, Z. Zhang, K. M. Thomas, R. Krishna and B. Chen, *J. Am. Chem. Soc.*, 2012, **134**, 8703-8710.
- F. Song, C. Wang, J. M. Falkowski, L. Ma and W. Lin, *J. Am. Chem. Soc.*, 2010, **132**, 15390-15398.
- A. M. Shultz, A. A. Sarjeant, O. K. Farha, J. T. Hupp and S. T. Nguyen, *J. Am. Chem. Soc.*, 2011, **133**, 13252-13255.
- C. Zhu, G. Yuan, X. Chen, Z. Yang and Y. Cui, *J. Am. Chem. Soc.*, 2012, **134**, 8058-8061.
- W. Xuan, C. Ye, M. Zhang, Z. Chen and Y. Cui, *Chem. Sci.*, 2013, **4**, 3154-3159.
- J. M. Falkowski, C. Wang, S. Liu and W. Lin, *Angew. Chem. Int. Ed.*, 2011, **50**, 8674-8678.
- J. M. DeSimone, *Science*, 2002, **297**, 799-803.
- P. J. Walsh, H. Li and C. A. de Parrodi, *Chem. Rev.*, 2007, **107**, 2503-2545.
- W. Xi, Y. Liu, Q. Xia, Z. Li and Y. Cui, *Chem. – Eur. J.*, 2015, **21**, 12581-12585.
- Y. N. Belokon, P. Carta, A. V. Gutnov, V. Maleev, M. A. Moskalenko, L. V. Yashkina, N. S. Ikonnikov, N. V. Voskoboev, V. N. Khrustalev and M. North, *Helv. Chim. Acta*, 2002, **85**, 3301-3312.
- P. Adão, J. Costa Pessoa, R. T. Henriques, M. L. Kuznetsov, F. Avecilla, M. R. Maurya, U. Kumar and I. Correia, *Inorg. Chem.*, 2009, **48**, 3542-3561.
- V. A. Blatov, A. P. Shevchenko and D. M. Proserpio, *Cryst. Growth Des.*, 2014, **14**, 3576-3586.
- K. S. W. Sing, D. H. Everett, R. A. W. Haul, L. Moscou, R. A. Pierotti, J. Rouquerol and T. Siemieniowska, *Pure Appl. Chem.*, 1985, **57**, 603-619.
- G. Leofanti, M. Padovan, G. Tozzola and B. Venturelli, *Catal. Today*, 1998, **41**, 207-219.

Journal Name

COMMUNICATION

25. K. B. Lee, M. G. Beaver, H. S. Caram and S. Sircar, *Ind. Eng. Chem. Res.*, 2008, **47**, 8048-8062.
26. S. Himeno, T. Komatsu and S. Fujita, *J. Chem. Eng. Data*, 2005, **50**, 369-376.
27. (a) V. Chechik, M. Conte, T. Dransfield, M. North and M. Omedes-Pujol, *Chem. Commun.*, 2010, **46**, 3372-3374; (b) Y. N. Belokon, M. North and T. Parsons, *Org. Lett.*, 2000, **2**, 1617-1619.
28. D. Dang, P. Wu, C. He, Z. Xie and C. Duan, *J. Am. Chem. Soc.*, 2010, **132**, 14321-14323.